The effect of start-up on energy recovery and compositional changes in brewery wastewater in bioelectrochemical systems

Johanna M. Haavisto[1,*], Marika E. Kokko[1], Aino-Maija Lakaniemi[1], Mira L. K. Sulonen[1,#], Jaakko A. Puhakka[1]

[1] *Tampere University, Faculty of Engineering and Natural Sciences, Tampere, Finland*

[#] *Present address: Universitat Autònoma de Barcelona, Departament Química, Biològica i Ambiental, Barcelona, Spain*

* Corresponding author: P.O. Box 541, FI-33104 Tampere University, Finland; E-mail: johanna.haavisto@tuni.fi; Telephone: +358400486070

Abstract

Start-up of bioelectrochemical systems (BESs) fed with brewery wastewater was compared at different adjusted anode potentials (-200 and 0 mV vs. Ag/AgCl) and external resistances (50 and 1000 Ω). Current generation stabilized faster with the external resistances (9±3 and 1.70±0.04 A/m^3 with 50 and 1000 Ω, respectively), whilst significantly higher current densities of 76±39 and 44±9 A/m^3 were obtained with the adjusted anode potentials of -200 and 0 mV vs. Ag/AgCl, respectively. After start-up, when operated using 47 Ω external resistance, the current densities and Coulombic efficiencies of all BESs stabilized to 9.5±2.9 A/m^3 and 12±2%, respectively, demonstrating that the start-up protocols were not critical for long-term BES operation in MFC mode. With adjusted anode potentials, two times more biofilm biomass (measured as protein) was formed by the end of the experiment as compared to start-up with the fixed external resistances. After start-up, the organics in the brewery wastewater, mainly sugars and alcohols, were transformed to acetate (1360±250 mg/L) and propionate (610±190 mg/L). Optimized start-up is required for prompt BES recovery, for example, after process disturbances. Based on the results of this study, adjustment of anode potential to -200 mV vs. Ag/AgCl is recommended for fast BES start-up.

Keywords

Adjusted anode potential, brewery wastewater, external resistance, microbial fuel cell, start-up protocol, process recovery

1. Introduction

Brewing industry produces on average 5.5 L of wastewater per 1 L of produced beer [1]. As the world wide beer production in 2014 was almost 200 Mm^3, the volume of produced brewery wastewater was close to 1000 Mm^3 [1,2]. Brewery wastewaters are concentrated (with chemical oxygen demand (COD) of 2000-6000 mg/L) and biodegradable (the ratio of biological oxygen demand (BOD) and COD being ~0.6), with pH close to neutral [3,4]. Brewery wastewaters are traditionally treated using aerobic, energy consuming biological processes such as activated sludge either in centralized municipal wastewater treatment plants or on-site [3,5]. Due to the high chemical energy content of the wastewater, biological treatments for energy recovery are of interest. For example, Chen et al. [6] produced methane (0.31 L CH_4/g-$COD_{removed}$) from brewery wastewater in a laboratory-scale membrane bioreactor, Zhuang et al. [7] reported 4.1 W/m^3 electricity production in a microbial fuel cell (MFC) with over 85% COD removal, and Estevam et al. [8] hydrogen production of 0.80-1.67 mol-H_2/mol-glucose.

MFCs are bioelectrochemical systems (BESs) in which organic compounds are oxidized and their chemical energy converted directly to electrical energy [9]. MFCs are promising for the pretreatment of brewery wastewater due to the high carbohydrate and low ammonium concentrations, while meeting the clean-up requirements set for of brewery wastewater likely needs combining bioelectrochemical pretreatment with aerobic or anaerobic post-treatment [3,10]. Recent studies with MFCs indicate that electricity production from wastewaters (0.097

kW/m^3) can partially or fully provide operating energy for the bioelectrochemical wastewater treatment (0.027 kW/m^3 needed for pumping) [10]. The advantages of MFCs in wastewater treatment compared to aerobic treatment are the low energy demand and the low excess sludge production [11]. Unlike anaerobic digestion, MFCs can successfully operate also at low-temperatures (20 °C and less) [12].

Wastewater composition varies highly between breweries [5] and, as brewing is a batch operation, the wastewater flow and composition fluctuate. Long interruptions in wastewater flow and washing detergents, for example, may change and inhibit microbial communities of BESs. A prompt recovery after disturbances is required to meet the overall treatment requirements [13]. However, start-up of BES is often time consuming and for this reason, several approaches for start-up have been studied. Using bioelectrochemical enrichment culture from a BES operated under similar conditions transferred as biomass from the biofilm or anolyte solution is considered as the fastest method for start-up [14–16]. Enrichment cultures can also be stored at + 4 °C as an anticipation for process disturbances [17]. Alternatively, anaerobic digester sludge [18–20], a combination of anaerobic sludge and enrichment culture [16], wastewater [10,14,21], rumen contents [22], sediment [22], or even activated sludge [20] can be used as the inoculum for start-up. The enrichment of electrochemically active microbial cultures can be supported electrochemically or chemically, e.g., with poised anode potential (stable or varied by maximum power point tracking method) [23,24] or suppressing methanogenesis by starvation [25], adding 2-bromomethanesulfonate [18], or by inducing oxygen stress [18]. However, the reports of using poised anode potential are contradictory [14,26]. Some studies report the highest current densities during the start-up with a more negative anode potentials [14,23] while other BESs performed best after more positive anode potentials [27,28]. Also, when BESs are started up using external resistance, some studies suggest that high external resistances (e.g. 1000 Ω) result in fast current production (compared to 100 Ω external resistance) [21], while others favored lower resistances (e.g. 5 Ω) to enable higher bacterial growth rates and current densities [29,30]. According to Logan et al. [31] the highest power densities can be obtained when the external resistance equals the internal resistance of the Ohmic resistance limited MFCs.

The efficiency of start-up depends on multiple factors such as the inoculum source, anode potential or external resistance, substrate, temperature, reactor design and electrode material [32]. The effect of start-up protocol on electricity generation under equal conditions after the start-up phase has been studied using acetate [33] or glucose [34] in well buffered media, but not with real wastewaters. With acetate, it was demonstrated that biofilm of a BES which was originally operated with a high external resistance, adapted to a low external resistances, which eliminated power overshoot [33]. With glucose, the start-up with +200 mV vs. Ag/AgCl accelerated the start-up more than 1000 Ω external resistance [34]. In addition to using direct electricity precursors (acetate) or other model compounds in start-up, studies with real wastewaters consisting of complex organic constituents are needed. Anaerobic treatment of real wastewaters requires sequential and interdependent reactions carried out by diverse anaerobic microbial community consisting of hydrolytic, fermentative as well as those donating electrons to the solid anode electrode [35]. Furthermore, start-up should be studied in less buffered systems. For this reason, the effect of start-up on subsequent electricity generation should be elucidated also with real wastewaters.

The purpose of this study was to optimize the BES start-up by comparing different poised anode potentials and external resistances, and to evaluate the influences of the different start-up

protocols on subsequent power production from brewery wastewater in MFC mode. The changes in wastewater composition and the biofilm formation on anode electrode were also determined. To the authors' knowledge, the effects of different poised anode potentials and external resistances on start-up and subsequent performance under equal conditions have not been previously studied with real wastewaters.

2. Materials and methods

2.1 BES construction and operation

Experiments were conducted in eight air-cathode BESs previously described by Cetinkaya et al. [19] with anode chamber volume of 123 mL. In this study, cation exchange membranes (CME 7000; 41 cm^2) were coated with Pt by spraying a mixture of 100 mg 20% Platinum on Vulcan XC-72R (E-TEK), 1 mL MQ, 3 mL isopropanol, 1 mL propanediol, and 0.807 mL 5% Nafion (Nafion® 117 solution, Aldrich) with an airbrush. This whole mixture was divided on eight membranes. Two carbon brush electrodes [36] were used as the anodes and two carbon cloth cathode electrodes (projected areas of 41 cm^2) were sandwiched between the Pt coated membranes and supporting frames on the both sides of the anode chamber (Fig. S1). Both anode electrodes and cathode electrodes were connected in parallel with titanium wires to form a single circuit. Anolyte with total volume of 500 mL was circulated (80 mL/min) over a recirculation bottle placed in 37 °C water bath. The recirculation maintained the BES temperature at ca. 29-30 °C. A reference electrode (BASi RE-5B Ag/AgCl) filled with 3 M NaCl (+204 mV vs. SHE at 30 °C) was positioned between the anode electrodes (Fig. S1).

The experiments were divided to a start-up phase and to a follow-up operation in MFC mode. The BESs were inoculated with fresh anaerobic sludge (50 mL) collected from a local municipal wastewater treatment plant (Viinikanlahti, Tampere, Finland). During the start-up phase (first 42 days), four different operational conditions were compared in duplicate BESs: operation with either 1000 Ω or 50 Ω external resistance, or anode potential adjusted to either 0 mV or -200 mV (against Ag/AgCl reference electrode). The BESs are hereafter referred to after the start-up protocols as: $BES_{1000\Omega}$, $BES_{50\Omega}$, BES_{0mV}, and BES_{-200mV}. During the follow-up operation in MFC mode (days 42-75), a 47 Ω external resistance was connected between anode and cathode in each of the BESs. The BESs were fed in 6-8 day intervals with diluted brewery wastewater (COD_{tot} 1410 ± 60 mg/L) buffered with $NaHCO_3$ (2 g/L).

To avoid the presence of inhibiting compounds, the wastewater was collected at the time of tank emptying from a local brewery. This brewery washes their lines and tanks with reusable acid and alkaline solutions and disinfect their tanks with peracetic acid, which will be oxidized on the surface of the tank. For the feedings, wastewater was mixed and divided to smaller batches to be stored at -20 °C to ensure constant quality at each feeding point. One wastewater batch was defrosted for every feeding. Wastewater characteristics (Table 1) were measured from one defrosted wastewater sample. During the start-up phase, feed solution COD was measured at every feeding point. After dilution with distilled water, the feed solution was flushed with nitrogen gas for 15 min to remove oxygen, and 330 mL of the buffered solution ($NaHCO_3$ dissolved in a mixture containing 70% wastewater and 30% distilled water) was inserted in a new recirculation bottle to replace the previous bottle to maintain the whole anolyte volume of

500 mL. Anolyte pH was measured manually twice between feedings and adjusted to 7 with 5 M NaOH, if pH was below 6.5.

Table 1. Composition of the brewery wastewater and the BES feed, i.e. diluted brewery wastewater with $NaHCO_3$ supplementation.

	Wastewater[a]	Feed solution[b]
pH	7.98	8.6 ± 0.3
COD_{tot}	1990 ± 80 mg/L	1410 ± 60 mg/L
COD_s	1950 mg/L	1370 mg/L
BOD_7	960 mg/L	670 mg/L
N_{tot}	10.3 mg/L	7.2 mg/L
PO_4^{3-}-P	31.3 mg/L	21.9 mg/L
Ethanol	516 mg/L	359 mg/L
Alkalinity	4.7 mM	3.3 mM
Sugars[c]	610 mg/L	430 mg/L
$NaHCO_3$		2.0 g/L
Conductivity	n.a.	2.53 ± 0.06 mS/cm

[a]Wastewater characteristics are reported as measured values; [b]Feed solution pH, COD_{tot} and conductivity are measured values, $NaHCO_3$ as added concentration, and others as calculated values; [c]Sugars are presented as glucose equivalents; n.a. = not analysed

2.2 Analyses and calculations

2.2.1 Electrochemical measurements and calculations

Potentiostat (DropSens µSTAT8000) was used for adjusting the anode potential (0 mV or -200 mV vs. Ag/AgCl) and measuring the current at 2 min intervals during the start-up phase so that anode electrodes were used as working electrodes, cathode electrodes as counter electrodes and reference electrode as a reference. All the anode potential values in the text are given as mV vs. Ag/AgCl. Cell voltages and anode potentials of the BESs operated in MFC mode with external resistances were recorded with Agilent 34970A data Acquisition/Switch Unit (Agilent, USA) at 2 min intervals. Current was calculated according to Ohm's law (I=U/R) and normalized against the anode chamber volume. To compare current production obtained during the different feedings, average current densities were calculated over each feeding cycle. Coulombic efficiency (CE) was calculated from the amount of COD (0.5 g) added during each feeding and electrical current data during the operation in MFC mode (days 56-63) according to Logan et al. [31]. Fed COD was used for the calculation of CE, as soluble COD was also released from the anaerobic sludge used as inoculum. Calculating the CE against removed COD would, thus overestimate the CE.

Linear sweep voltammetry (LSV) was done using a potentiostat (Palmsens3, Netherlands) for anode electrodes after the start-up phase (day 42) and in the end of the operation in MFC mode (day 71). Scan rate was 0.5 mV/s and the scan ranged from -550 mV to +200 mV (vs. Ag/AgCl). Measurements were started after 30 min stabilization in open circuit mode one day after the

previous feeding. The anodic LSV measurement was followed by whole cell LSV starting from 5-50 mV above open cell voltage towards +5 mV at 0.2 mV/s scan rate. Internal resistance of the MFC was estimated from the whole cell LSV data ($R_{internal}$ = U/I) based on the current and voltage at the maximum power point [31].

2.2.2 Chemical analyses

Anolyte samples were taken for chemical analyses from the circulation bottles three times a week. Samples were filtered through 0.2 µm polyester filters and stored at -20 °C for sugar and volatile fatty acid (VFA) analyses. Anolyte pH and conductivity were measured from fresh samples with WTW pH 330 meter and WTW InoLab Level 1 Multimeter, respectively. Sugar concentration was measured as glucose equivalents using phenol-sulphuric acid method [37]. Method was modified by decreasing the sample volume from 2 mL to 1 mL and reagent volumes from 1 mL to 0.5 mL (5% phenol solution) and from 5 mL to 2.5 mL (sulphuric acid). VFA (acetate, propionate, butyrate, isobutyrate, and valeric acid) and alcohol (ethanol and butanol) concentrations were measured with a gas chromatograph equipped with a flame ionization detector as described by Haavisto et al. [38].

Wastewater alkalinity was analysed according to the Finnish standard SFS 3005 by titrating the sample with 0.10 M HCl to pH 4.5. N_{tot} and PO_4^{3-}-P were measured using HACH LANGE kits (LCK 238 for N_{tot} and LCK 349 for PO_4^{3-}-P) according to the manufacturer´s instructions. BOD_7 was measured with WTW OxiTop measuring system from appropriately diluted samples according to the manufacturer's instructions (Application report O2 500231). COD was measured with the dichromate method according to the Finnish standard SFS 5504 (1988). Soluble COD (COD_s) refers to values measured from filtered (0.2 µm) samples. Cumulative effluent acetate and propionate and fed COD (in section 3.3 and Figure S3) were calculated based on the sum of produced acetate and propionate (as COD equivalents) and sum of COD fed after the first feeding. Decreased anolyte volumes in the end of the feeding cycles due to evaporation (19 ± 7% per feeding) were considered when calculating the acetate and propionate accumulation. Acetate and propionate originated from the degrading organic components of anaerobic sludge (used as inoculum) and brewery wastewater. Acetate and propionate were converted to theoretical COD (1.0667 $g_{COD}/g_{acetate}$ and 1.5135 $g_{COD}/g_{propionate}$) according to Van Haandel and Van der Lubbe [39].

2.2.3 Microbial culture analyses

Analyses for total microbial quantity and microbial community composition were conducted from anode biofilms in the end of the experiment (day 75). Biofilm was sequentially removed from the anode electrodes in laminar flow hood by mechanically scrubbing the carbon brush electrodes against each other as long as biomass was visibly detaching to a small volume (10-20 mL) of sterile 0.9% NaCl solution in 50 mL Falcon tube. The overall solution with detached biomass was collected (80-120 mL) and concentrated by centrifuging (5000 x g, 10 min). Centrifugated biomass samples (15 mL) were divided into microbial community samples (4 mL) and biomass samples (11 mL) and both samples were frozen (-20 °C). Mechanical scrubbing was selected as the biofilm separation method based on previous experiments. From the different biomass detachment methods used in the previous testing mechanical scrubbing resulted in

highest quantity of detached biomass and thus allowed the most reliable comparison of biomasses between different reactors.

Frozen biomass samples were freeze-dried (Christ Alpha 1-4 LD plus, Germany) and weighed to determine the quantity of the biomass. Bio-Rad Protein Assay (based on Bradford method) was used for measuring the protein mass on anode as bovine serum albumin (BSA) equivalents. Triplicate samples (approximately 0.01 g of dry sample mixed with 100 µL distilled water) were analyzed according to the manufacturer's standard procedure instructions using UV-VIS spectrophotometer (Shimadzu UV-1700) for absorbance measurement. For protein mass calculation, the biomass dry weight was corrected by multiplying the mass with 1.36 to take into account the share of microbial community samples removed before freeze drying. Then the protein mass was calculated from the corrected biomass dry weights and the protein concentrations.

Microbial community was profiled as previously described by Haavisto et al. [38]. PowerSoil DNA isolation kit (MO BIO Laboratories, Inc., Carlsbad, CA, USA) was used for DNA extraction followed by partial 16S rRNA gene PCR amplification with GC-BacV3f [40] and 907r [41] primers as described by Koskinen et al. [42]. DNA sequences were separated with denaturing gradient gel electrophoresis (DGGE) as described by Lakaniemi et al. [43], reamplified according to Koskinen et al. [42], and sequenced at Macrogen Inc. (Seoul, Korea). Analyzed sequence data (BioEdit software) was compared to known sequences with BLAST (https://blast.ncbi.nlm.nih.gov/Blast.cgi).

3. Results and discussion

3.1 BES start-up

BESs were fed in semi-continuous mode with brewery wastewater under the different start-up conditions and their performances were monitored as current densities (Fig. 1) and as linear sweep voltammograms (Fig. 2). During the first feeding, high peak currents were detected due to biological oxidation of organic compounds in the anaerobic sludge used as the inoculum. The lowest current densities were measured during the 2nd feeding, after which the current densities increased and the highest average current densities were obtained during the last (6th) feeding. The highest average current densities obtained with BES_{-200mV} and BES_{0mV} were 76 ± 39 and 44 ± 9 A/m^3, respectively (Fig. 1). With $BES_{50\Omega}$ (anode potential -463 ± 14 mV) and $BES_{1000\Omega}$ (anode potential -480 ± 6 mV), the highest average current densities were 9 ± 3 and 1.70 ± 0.04 A/m^3, respectively. According to Wei et al. [44], higher anode potential should increase the current production because electrochemically active microorganisms gain more energy for growth, but only if those bacteria are able to utilize the anode at higher potential as an electron acceptor [26]. This can be affected e.g. by the available substrate [45] and the electron transfer mechanisms of the bacteria enriched in the biofilm [14,23]. Our results show higher current at lower anode potential of -200 mV compared to 0 mV. Also Aelterman et al. [46] reported higher current densities with -200 mV vs. Ag/AgCl adjusted anode potential (compared to 0 and -400 mV) in an acetate-fed BES.

The current production stabilized faster in the BESs with the external resistances, but the obtained maximum average current densities were significantly lower (Fig. 1) than in the BESs

with the adjusted anode potential. In the last two feeding cycles, current densities increased by 25 and 38 A/m^3, 15 and 21 A/m^3, 1.3 and 0.32 A/m^3, and 0.37 and 0.068 A/m^3 in BES_{-200mV}, BES_{0mV}, $BES_{50\Omega}$, and $BES_{1000\Omega}$, respectively. This is in contrast to the results of Wang et al. [34] who reported faster start-up with adjusted anode potential (+200 mV) compared to 1000 Ω external resistance in terms of current production stabilization. In addition, Hong et al. [33] and Ahn et al. [21] reported faster current generation stabilization in terms of reproducible current cycles with higher external resistance, but in this study the current generation stabilization time was similar with high and low external resistances. The start-up phase was finished in the end of the 6^{th} feeding once the current generation was stabilized with $BES_{50\Omega}$ and $BES_{1000\Omega}$ to allow the comparison of different start-up protocols after minimal start-up duration. The immediate increase in current density after feeding (Fig. S2) indicates, according to Carmona-Martinez et al. [47], that the start-up phase was sufficient for the development of a mature electrochemically active biofilm.

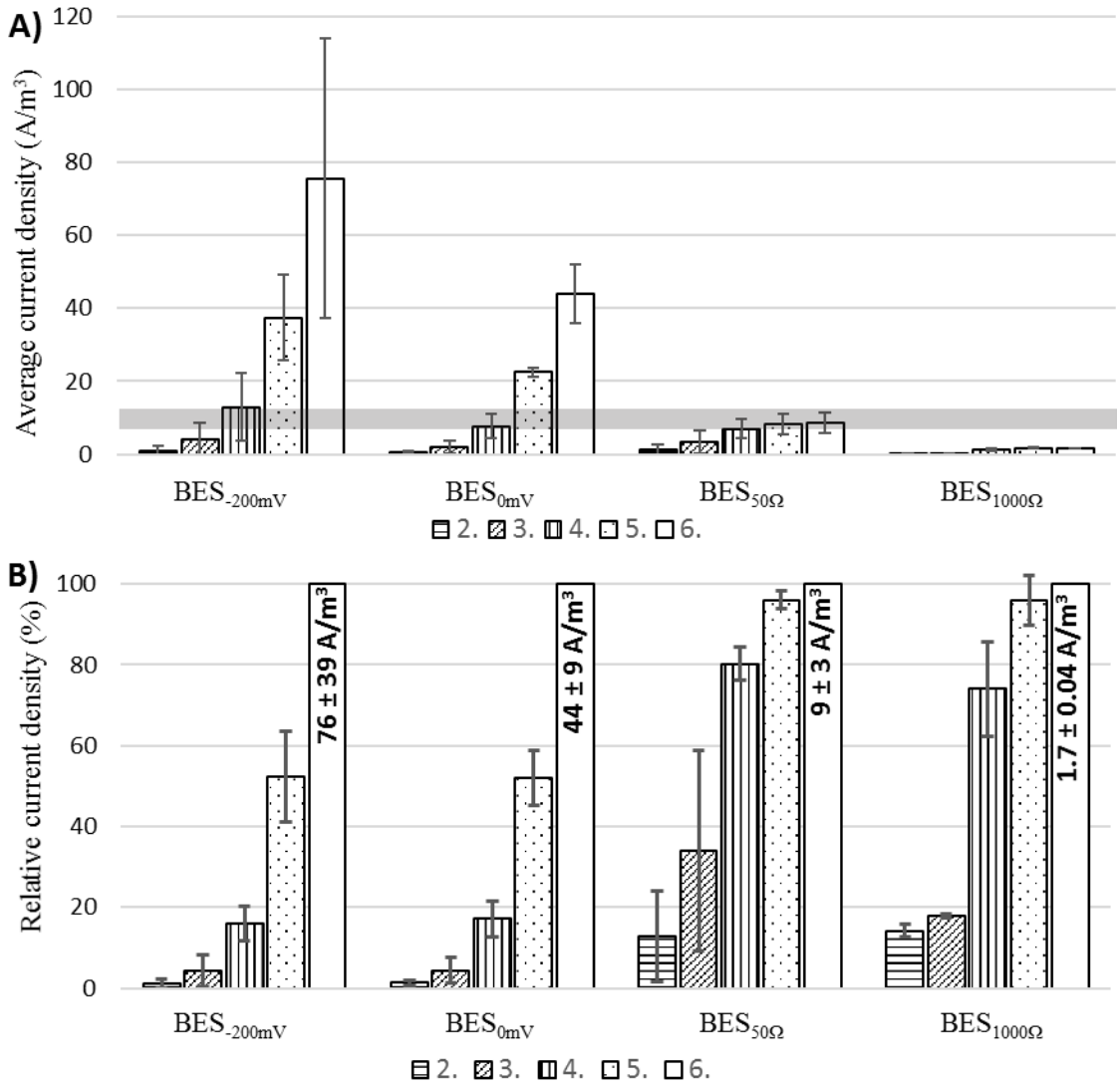

Fig. 1. Average current densities during the start-up of BESs fed in semi-continuous mode with brewery wastewater. The bars show A) current densities (A/m^3) of the feedings 2 – 6 and B) the relative current densities (%) of the feedings 2 – 5 calculated against the average current densities of the last (6th) feeding (=100%) for the different start-up protocols. Standard deviations indicate the differences between duplicate reactors. The shaded area of current densities in A) represents the stable current density (9.5 ± 2.9 A/m^3) obtained during the subsequent operation in MFC mode after the start-up phase.

In the end of the start-up phase, the performances of the BESs were compared using anodic LSVs (Fig. 2). The maximum current obtained in the LSV decreased in the same order, i.e. from BES_{-200mV}, BES_{0mV}, $BES_{50\Omega}$ to $BES_{1000\Omega}$, as did the highest average current densities obtained during the last start-up phase feeding (Fig. 1). The highest current in the BES_{-200mV} exceeded the maximum current measurable with the potentiostat (30 mA), while with BES_{0mV}, $BES_{50\Omega}$ and $BES_{1000\Omega}$ the highest currents were 26.4, 9.9, and 1.9 mA (215, 80, and 15 A/m^3), respectively. While power overshoot was observed at anode potentials of -340, -300 and 50 mV in the

$BES_{1000\Omega}$, $BES_{50\Omega}$ and BES_{0mV}, respectively, no power overshoot was detected with BES_{-200mV} (Fig. 2). Previous studies have shown overshoots at lower anode potentials and current values on anodic cyclic voltammetry curves in the BESs operated with high external resistance [33] or highly negative anode potential [48] due to the electroactive community not being able to produce high currents under given conditions. LSV curves in this study indicate that earlier adaptation of microbial cultures to higher current enabled higher current production on varying anode potentials.

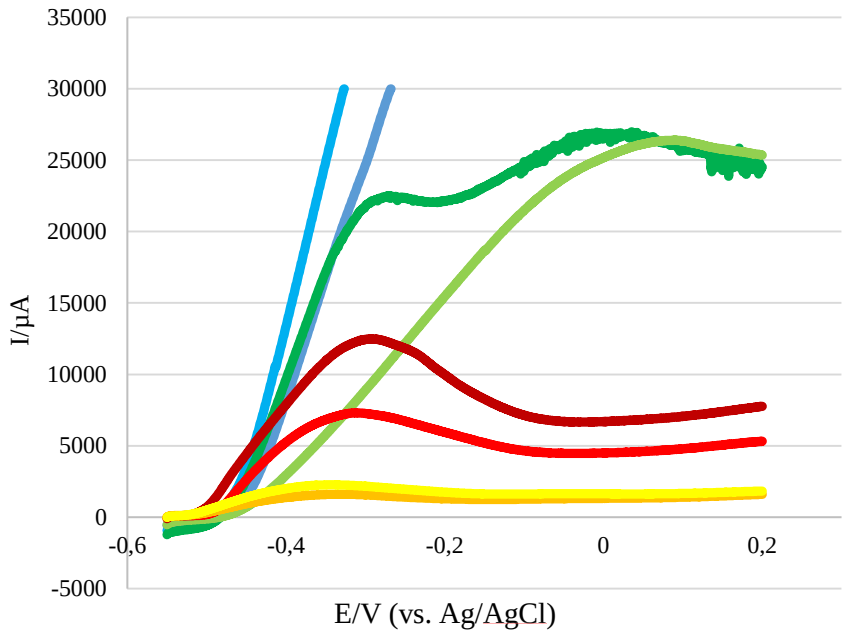

Fig.2. Anodic linear sweep voltammograms after operating semi-continuous brewery wastewater fed BESs with the different start-up protocols for 42 d. The results with different colors represent the duplicate reactors with studied start-up protocols: blue for BES_{-200mV}, green for BES_{0mV}, red for $BES_{50\Omega}$ and yellow and orange for $BES_{1000\Omega}$. The current (µA) values of BES_{-200mV}_1 and BES_{-200mV}_2 exceeded the measuring range of the potentiostat (30 mA) with anode potentials higher than -326 mV and remained at or above 30 mA at more positive anode potentials.

3.2 Performance after start-up

After the start-up, all BESs were operated in MFC mode for 28 days with 47 Ω external resistance (Table 2), which was close to the internal resistance (59 Ω) of the BES producing the highest current (BES_{-200mV}_1) at the end of the start-up. The start-up protocol with adjusted anode potential of -200 mV (BES_{-200mV}) provided the highest average current density (10.6 A/m^3) in the beginning of the follow-up operation period. The current density, however, decreased to 9.7 A/m^3 towards the end of the operation (days 63-70). With $BES_{1000\Omega}$, after the current densities of 1.7 ± 0.04 A/m^3 during start-up, the current density increased to 9.2 A/m^3 (Table 2). At the end of the operation, the current densities were similar in all the BESs (9.2-9.7 A/m^3) despite the different start-up protocols. The results are in accordance with Wang et al.

[34], who showed that after start-up protocols of +200 mV anode potential and 1000 Ω external resistance, the cell voltages at same conditions (1000 Ω external resistance) became similar (641 ± 4 mV after 11 days). The highest power density in our study (0.51 ± 0.03 W/m^3) was lower compared to other results obtained with brewery wastewater (1.3 W/m^3 [49] at pH 7 and 35 °C, and 4.1 W/m^3 at 30 °C [7]). This was because our semi-continuous BES with air-cathode was not optimal for electricity production, which is also indicated by the high VFA concentrations in the effluent (see section 3.3). Higher power densities could likely have been obtained by choosing an external resistance close to the internal resistance for each of the BES individually. The electrical energy yield was 84 kJ/kg$_{\text{fed COD}}$ (calculated for 0.51 W/m^3 power density), which is slightly lower compared to 110 and 120 kJ/kg$_{\text{fed COD}}$ obtained by Dong et al. [10] and Lu et al. [50] in 90 and 20 L brewery wastewater treating MFCs, respectively, but almost tenfold higher compared to MFCs fed with liquid fraction of municipal solid waste after solid-liquid separation (8-9 kJ/kg$_{\text{removed COD}}$) [51].

Table 2. The effect of different start-up protocols on internal resistance, current densities and anode potentials. Internal resistance was measured at the end of the start-up phase and after the subsequent follow-up operation (calculated from whole cell polarization curves, Fig. S3), and average current densities and anode potentials were measured at the beginning (7th feeding) and at the end (10th feeding) of the operation in MFC mode with 47 Ω external resistance.

	After start-up	In the end of the operation	7th feeding[a]		10th feeding[b]	
	Internal resistance (Ω)	Internal resistance (Ω)	Avg. current density (A/m^3)	Avg. anode potential (mV)	Avg. current density (A/m^3)	Avg. anode potential (mV)
BES$_{-200mV}$	71 ± 16	86 ± 15	10.6 ± 1.1	-460 ± 12	9.7[c]	-481[c]
BES$_{0mV}$	109 ± 15	140 ± 27	8.6 ± 0.7	-452 ± 4	9.2 ± 2.1	-469 ± 19
BES$_{50Ω}$	156 ± 52	177 ± 65	7.9 ± 3.1	-454 ± 19	9.4 ± 2.7	-476 ± 15
BES$_{1000Ω}$	203 ± 41	121[c]	6.7[c]	-437[c]	9.2[c]	-466[c]

[a] days 43-50; [b] days 63-70; [c] results from only one replicate due to connection problems

In the end of the experiment (day 71), power overshoot was visible in the anodic LSVs (Fig. 3) in all BESs at anode potentials between -220 and -300 mV and the shapes of the LSV curves resembled those obtained in the anodic LSV of BES$_{50Ω}$ during the start-up phase (Fig. 2). The highest current value on LSV curve with BES$_{50Ω}$ decreased from 9.9 during start-up (day 42) to 8.0 mA during the operation with 47 Ω presumably due to decreased conductivity (from ca. 4-5 to ca. 3 mS/cm). With BES$_{1000Ω}$, the highest current in the anodic LSV increased from 1.9 to 11.7 mA, and with BES$_{0mV}$ it decreased from 26.5 to 11.8 mA. The highest anodic LSV current of BES$_{-200mV}$ reactors was 13.5 mA on day 71. The changes in the anode potentials where the peak current is achieved (Figs. 2 and 3) may be due to changes in the quantity or type of redox active enzymes synthetized by electrochemically active microbes [33]. In anodic LSVs, the higher maximum current (13.5 mA compared to 8.0-11.8 mA) at same or more negative anode potential (at -300 mV compared to -300 - -220 mV) demonstrates smaller overpotential with

BES_{-200mV} compared to the other start-up protocols (Fig. 3). However, the differences in maximum currents on day 71 were small compared to the differences right after the start-up on day 42 (Fig. 2). Thus, the start-up protocol had an insignificant effect on LSV curve during the follow-up operation as previously reported by Hong et al. [33].

Both the average current densities (Table 2) and the LSV curves (Fig. 3) showed that the start-up protocol did not significantly affect the current production in BESs after 30 d operation with selected external resistance after the start-up phase. Thus, the start-up phase should aim mainly at accelerating the biofilm development rather than producing maximum current.

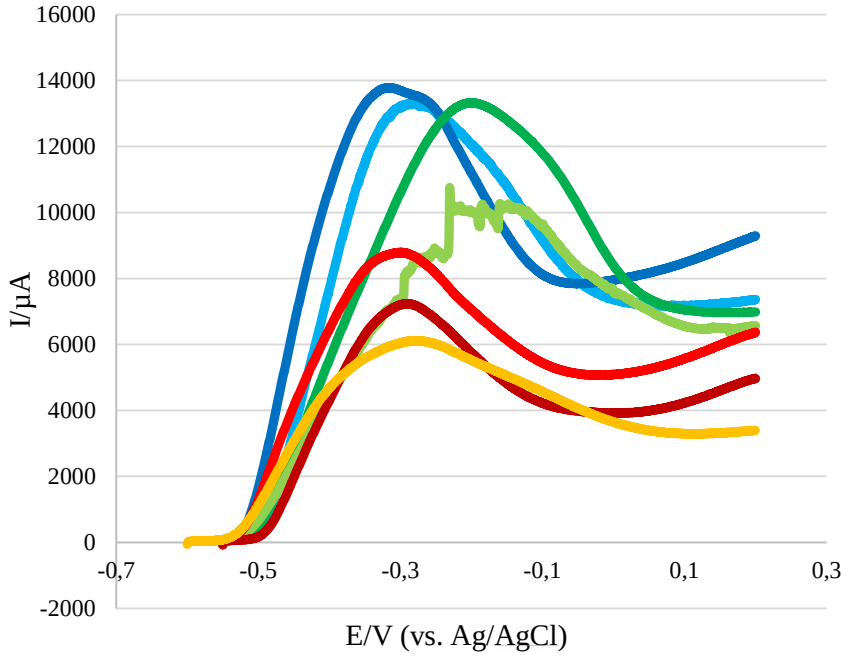

Fig. 3. Anodic linear sweep voltammograms measured in the end of the experiment (day 71) after operating the BESs in MFC mode (with 47 Ω resistance) for 29 days. The results with different colors represent the duplicate reactors with studied adjusted anode potentials or external resistances used as start-up protocols in the start-up phase (days 0-42): blue for BES_{-200mV}, green for BES_{0mV}, red for $BES_{50\Omega}$ and orange for $BES_{1000\Omega}$. Due to connection problems, the results of $BES_{1000\Omega}$_2 are not shown.

3.3 Transformation of wastewater organics during and after start-up

Sugars and alcohols were almost completely removed (>96% sugar removal and no alcohols were detected in the effluent) from the diluted brewery wastewater during both the start-up and the subsequent follow-up operation phases. During the start-up phase, VFA accumulated in BESs during all the feedings (Figs. 4. and S3). The highest concentrations were detected at the end of the 2nd feeding after which VFA concentrations decreased towards the end of the start-up phase (Table 3). VFA accumulation was similar with all start-up protocols in the end of both the start-up and the follow-up operation (Table 3) with acetate and propionate contributing the most of the

VFAs, whilst also butyrate (≤ 321 mg/L) and valerate (≤ 251 mg/L) were detected in some samples. In the end of the start-up phase, the acetate and propionate concentrations were in the range of 1100-1300 mg/L and 630-680 mg/L, respectively. Highest acetate (2800-4700 mg/L) and propionate (1200-2200 mg/L) concentrations at the end of 2nd feeding of the start-up phase likely originated from degradation of the anaerobic sludge used as inoculum. The anaerobic sludge inoculum (10% v/v) attached to the carbon brush anode electrodes. The sludge was partially hydrolyzed during the incubation especially during the start-up phase (first five batch cycles), increasing the soluble COD concentrations. Although the COD from the anaerobic sludge hydrolysis likely affected the BES performance, it did not compromise the comparison of the different start-up protocols. During the follow-up phase, Coulombic efficiency (CE) calculated for the fed COD was 12 ± 2% (on days 56-63), which is of the same order as results of Wen et al. (<10%) and Zhuang et al. (6.3-7.6%; calculated for removed COD) reported for brewery wastewater [7,52].

Table 3. The organic compounds present in the diluted brewery wastewater (feed solution) and BES effluents after the start-up phase (day 42) and the follow-up period (day 70). Standard deviations stand for differences between duplicate BESs.

Sample	Start-up protocol	Acetate (mg/L)	Propionate (mg/L)	Sugars (mg/L)	Ethanol (mg/L)[a]
Feed solution		0	0	430	360
Effluent from the end of the start-up phase	BES_{-200mV}	1100 ± 600	680 ± 80	10.9 ± 1.1	n.d.[b]
	BES_{0mV}	1120 ± 140	670 ± 150	9.7 ± 1.0	n.d.
	$BES_{50\Omega}$	1200 ± 200	630 ± 50	9.3 ± 1.1	n.d.
	$BES_{1000\Omega}$	1290 ± 120	650 ± 150	13 ± 6	n.d.
Effluent from the end of the follow-up operation	BES_{-200mV}	1170 ± 70	420 ± 140	10 ± 3	n.d.
	BES_{0mV}	1100 ± 200	500 ± 200	14 ± 3	n.d.
	$BES_{50\Omega}$	1400 ± 200	480 ± 130	12.2 ± 1.1	n.d.
	$BES_{1000\Omega}$	1270 ± 50	400 ± 100	13.4 ± 1.5	n.d.

[a] Detection limit for ethanol was 80 mg/L; [b] n.d. not detected

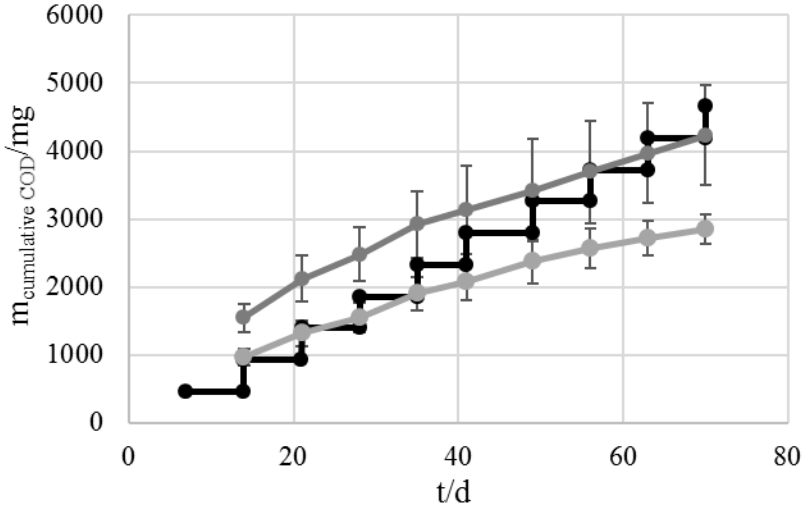

Fig. 4. Cumulative acetate (grey) and propionate (light grey) formation as COD equivalents in BES_{-200mV} after the first feeding. Cumulative fed COD (measured average feed solution COD) is shown in black as a reference. Higher concentrations of acetic acid and propionic acid compared to the fed COD are due to acetate and propionate production from the anaerobic sludge used as inoculum. COD accumulation with the other start-up protocols is shown in Fig. S4.

The low COD removal (Fig. 4) and current densities (Table 2) demonstrate that the studied BESs were not optimal for current production, but the efficient conversion of organic compounds from the wastewater to simple VFAs (Fig. 5) indicate that BESs are promising for pretreatment of brewery wastewater due to simultaneous degradation of organic compounds and current production. The highest COD removal efficiency reported from brewery wastewater has been 95% [50] showing that high COD removal from brewery wastewater is attainable with process optimization. In addition, optimizing the BES for current production would likely enable more efficient removal of VFAs and higher production of current. The accumulation of VFAs in MFCs was also reported by Chandrasekhar & Mohan [53] during bioelectrochemical pretreatment of food waste for dark fermentation. During the follow-up operation in MFC mode in this study, almost 90% of the effluent COD was acetate and propionate in all the BESs (Fig. 5). This would be suitable influent composition for anaerobic digestion as the VFA concentrations remained well below inhibitory to methanogens (13 g/L acetate and 3.5 g/L propionate) [54].

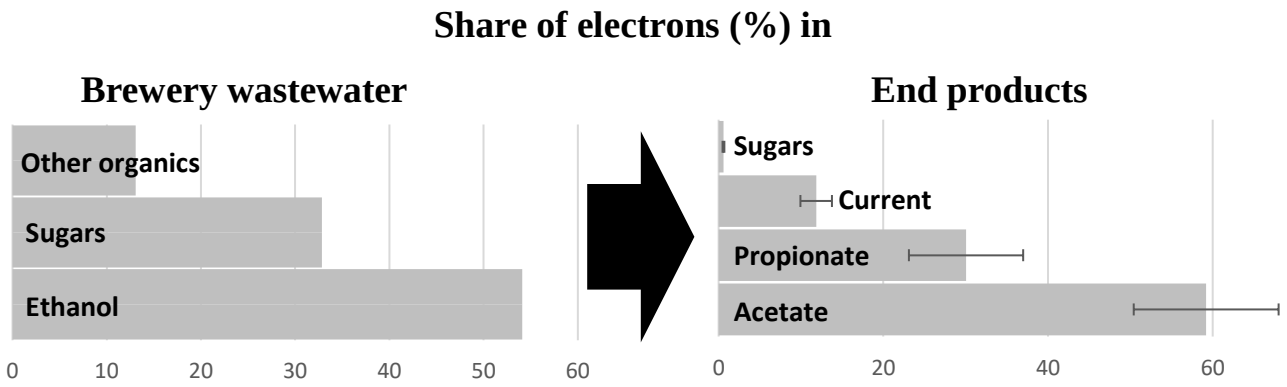

Fig. 5. Fate of electrons (%) in BES fed with brewery wastewater in the end of the BES operation in MFC mode. The bars represent the COD components of the brewery wastewater (on the left), and the average values of transformation products in the effluents of all BES on day 63 (on the right). The term current indicates the share of electrons recovered as electrical current.

3.4 Biomass accumulation and microbial community composition on the BES anodes

Biomass accumulation and community composition on the BES anodes was determined on day 75 at the end of the operation of the BESs in MFC mode (Fig. 6, and Fig. S6), because it was not possible to take biofilm samples from the carbon brush anodes during the operation. The highest protein quantity of 1.6-1.7 mg/BES was detected from BES anodes started up with the adjusted anode potentials (BES_{0mV} and BES_{-200mV}). Approximately 50% less protein (0.6-0.8 mg/BES) accumulated on the anodes of the BESs started up with the fixed external resistances. Higher anode potentials (at certain potential range, which is dependent on e.g. microbial community and substrate) are associated with higher biomass yields due to more energy available for microbial growth [27], which is in agreement with our study (anode potentials in $BES_{50\Omega}$ and $BES_{1000\Omega}$ were between -463 and -480 mV). To evaluate the effect of average current density on biomass, the biomass was illustrated as a function of the average current densities calculated over the feeding cycles 2-10 (Fig. S5), which clearly shows that anodic biomass increased with average current densities. The higher biomass production accompanied with higher current densities was well in accordance with the results by Aelterman et al. [46] reporting approximately 50% higher mass of biofilm with 0 and -200 mV anode potentials than with -400 mV (vs. Ag/AgCl) anode potential on day 22.

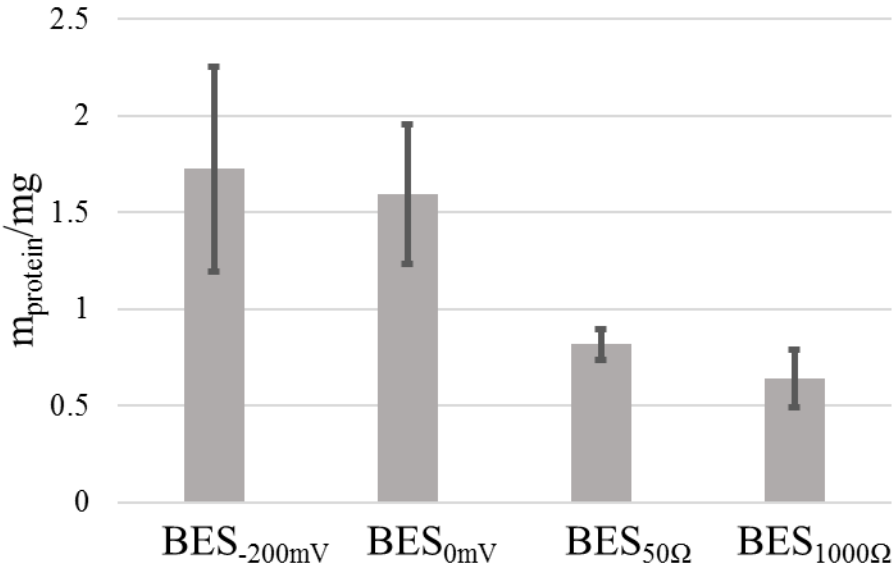

Fig. 6. Protein mass (mg) as bovine serum albumin (BSA) equivalents on an MFC anode electrodes (2x carbon brush: Length 5.5 cm, diameter 2.5 cm). Standard deviations show the differences between duplicate BESs.

Anaerobic sludge from municipal wastewater treatment plant is a rich source of microorganisms capable of utilizing a complex range of different substrates [55]. It is also known to contain electrochemically active microorganisms [20]. Anaerobic sludge was, therefore, used as inoculum in this study to support the conversion of different brewery wastewater constituents to electricity. As indicated by functional changes in electricity generation, phylogenetically very diverse microbial communities were enriched differently during the start-up under the different selection pressures of BES_{-200mV}, BES_{0mV}, $BES_{50\Omega}$ and $BES_{1000\Omega}$. This resulted in considerably different process and start-up performances.

The microbial communities were analyzed on day 75 after operating the BESs in MFC mode for 33 days with the same external resistance. Based on qualitative PCR-DGGE analysis (Table S1), in the end of the follow-up operation the anode electrodes were occupied by several known electrochemically active bacteria: *Klebsiella* sp., *Citrobacter* sp., *Azonexus* sp., *Escherichia coli*, and *Geobacter* sp. [35,56–58]. The fermentative bacteria of the biofilm samples included *E. coli* and *Selenomonas* sp. [59]. *E. coli* and *Citrobacter* sp., as facultative anaerobes, consumed oxygen potentially penetrating through CEM of the air-cathode reactor [57]. Only minor differences in community compositions were seen both between the duplicate MFCs and between different start-up protocols. Thus, no significant effects on the final anodic microbial community could be associated with the different start-up protocols (Fig. S6).

Microbial communities in anaerobic sludge remain viable and diverse for long periods [60]. Electricity generation in this study was different in the end of the studied start-up protocols indicating different community profiles. However, the operation under equal selection pressure (i.e. external resistance of 47 Ω) after the start-up period for 33 days resulted in enrichment of microbial communities into similar direction. For example, Ishii et al. [61] have reported

variation in the abundance of the bacteria in different classes during the long term BES operation, which supports the conclusion that in this study the similar selection pressure in BESs after the start-up affected the final microbial communities at anodes.

4. Conclusions

Among the studied start-up protocols (-200 mV and 0 mV vs. Ag/AgCl adjusted anode potentials and 50 Ω and 1000 Ω external resistances), -200 mV accelerated the current production most in air-cathode BES fed with brewery wastewater, with the highest average current density of 76 ± 39 A/m^3. Adjusted anode potentials of 0 and -200 mV enhanced the anode biofilm growth more than external resistances of 50 and 1000 Ω. High volatile fatty acids accumulation and low (12 ± 2%) Coulombic efficiency show that further optimization of the BES reactor configuration is needed to enhance the conversion of the organic content of the brewery wastewater into current. The results indicate that of the tested methods, the most optimal for efficient BES start-up is adjusted anode potential of -200 mV. The start-up conditions did not affect electricity production or microbial community composition in long-term BES operation, but are considered critical for fast recovery after process disturbances.

Acknowledgements

This work was supported by the Academy of Finland (New Indigo ERA-Net Energy 2014; Project no. 283013) and Maa- ja vesitekniikan tuki ry -foundation.

Declarations of interest: none

References

[1] Punda I. Agribusiness Handbook. FAO; 2009.

[2] Food and Agriculture Organization of the United Nations. FAOSTAT 2018. http://www.fao.org/faostat/en/#data/QD/visualize (accessed January 16, 2019).

[3] Simate GS, Cluett J, Iyuke SE, Musapatika ET, Ndlovu S, Walubita LF, et al. The treatment of brewery wastewater for reuse: State of the art. Desalination 2011;273:235–47. doi:10.1016/j.desal.2011.02.035.

[4] Rao AG, Reddy TSK, Prakash SS, Vanajakshi J, Joseph J, Sarma PN. pH regulation of alkaline wastewater with carbon dioxide: A case study of treatment of brewery wastewater in UASB reactor coupled with absorber. Bioresour Technol 2007;98:2131–6. doi:10.1016/j.biortech.2006.08.011.

[5] Arantes MK, Alves HJ, Sequinel R, da Silva EA. Treatment of brewery wastewater and its use for biological production of methane and hydrogen. Int J Hydrogen Energy 2017;42:26243–56. doi:10.1016/j.ijhydene.2017.08.206.

[6] Chen H, Chang S, Guo Q, Hong Y, Wu P. Brewery wastewater treatment using an anaerobic membrane bioreactor. Biochem Eng J 2016;105:321–31. doi:10.1016/j.bej.2015.10.006.

[7] Zhuang L, Yuan Y, Wang Y, Zhou S. Long-term evaluation of a 10-liter serpentine-type microbial fuel cell stack treating brewery wastewater. Bioresour Technol 2012;123:406–12. doi:10.1016/j.biortech.2012.07.038.

[8] Estevam A, Arantes MK, Andrigheto C, Adriana F, da Silva EA, Alves HJ. Production of biohydrogen from brewery wastewater using Klebsiella pneumoniae isolated from the environment. Int J Hydrogen Energy 2018;43:4276–83. doi:10.1016/j.ijhydene.2018.01.052.

[9] Pant D, Singh A, Van Bogaert G, Olsen SI, Nigam PS, Diels L, et al. Bioelectrochemical systems (BES) for sustainable energy production and product recovery from organic wastes and industrial wastewaters. RSC Adv 2012;2:1248–63. doi:10.1039/c1ra00839k.

[10] Dong Y, Qu Y, He W, Du Y, Liu J, Han X, et al. A 90-liter stackable baffled microbial fuel cell for brewery wastewater treatment based on energy self-sufficient mode. Bioresour Technol 2015;195:66–72. doi:10.1016/j.biortech.2015.06.026.

[11] Rabaey K, Lissens G, Siciliano SD, Verstraete W. A microbial fuel cell capable of converting glucose to electricity at high rate and efficiency. Biotechnol Lett 2003;25:1531–5.

[12] Pham TH, Rabaey K, Aelterman P, Clauwaert P, De Schamphelaire L, Boon N, et al. Microbial fuel cells in relation to conventional anaerobic digestion technology. Eng Life Sci 2006;6:285–92. doi:10.1002/elsc.200620121.

[13] Butti SK, Velvizhi G, Sulonen MLK, Haavisto JM, Koroglu EO, Cetinkaya AY, et al. Microbial electrochemical technologies with the perspective of harnessing bioenergy: Maneuvering towards upscaling. Renew Sustain Energy Rev 2016;53:462–76. doi:10.1016/j.rser.2015.08.058.

[14] Zhang F, Xia X, Luo Y, Sun D, Call DF, Logan BE. Improving startup performance with carbon mesh anodes in separator electrode assembly microbial fuel cells. Bioresour Technol 2013;133:74–81. doi:10.1016/j.biortech.2013.01.036.

[15] Liu Y, Harnisch F, Fricke K, Sietmann R, Schröder U. Improvement of the anodic bioelectrocatalytic activity of mixed culture biofilms by a simple consecutive electrochemical selection procedure. Biosens Bioelectron 2008;24:1006–11. doi:10.1016/j.bios.2008.08.001.

[16] Dessì P, Porca E, Haavisto J, Lakaniemi A-M, Collins G, Lens PNL. Composition and role of the attached and planktonic microbial communities in mesophilic and thermophilic xylose-fed microbial fuel cells. RSC Adv 2018;8:3069–80. doi:10.1039/c7ra12316g.

[17] Haavisto JM, Lakaniemi AM, Puhakka JA. Storing of exoelectrogenic anolyte for efficient

548 microbial fuel cell recovery. Environ Technol (United Kingdom) 2019;40:1467–75.
549 doi:10.1080/09593330.2017.1423395.

550 [18] Chae KJ, Choi MJ, Kim KY, Ajayi FF, Park W, Kim CW, et al. Methanogenesis control
551 by employing various environmental stress conditions in two-chambered microbial fuel
552 cells. Bioresour Technol 2010;101:5350–7. doi:10.1016/j.biortech.2010.02.035.

553 [19] Cetinkaya AY, Ozdemir OK, Demir A, Ozkaya B. Electricity Production and
554 Characterization of High-Strength Industrial Wastewaters in Microbial Fuel Cell. Appl
555 Biochem Biotechnol 2017;182:468–81. doi:10.1007/s12010-016-2338-7.

556 [20] Gao C, Wang A, Wu W-M, Yin Y, Zhao Y-G. Enrichment of anodic biofilm inoculated
557 with anaerobic or aerobic sludge in single chambered air-cathode microbial fuel cells.
558 Bioresour Technol 2014;167:124–32. doi:10.1016/j.biortech.2014.05.120.

559 [21] Ahn Y, Logan BE. Domestic wastewater treatment using multi-electrode continuous flow
560 MFCs with a separator electrode assembly design. Appl Microbiol Biotechnol
561 2013;97:409–16. doi:10.1007/s00253-012-4455-8.

562 [22] Dennis PG, Virdis B, Vanwonterghem I, Hassan A, Hugenholtz P, Tyson GW, et al.
563 Anode potential influences the structure and function of anodic electrode and electrolyte-
564 associated microbiomes. Sci Rep 2016;6:1–11. doi:10.1038/srep39114.

565 [23] Torres CI, Krajmalnik-Brown R, Parameswaran P, Marcus AK, Wanger G, Gorby YA, et
566 al. Selecting Anode-Respiring Bacteria Based on Anode Potential : Phylogenetic ,
567 Electrochemical , and Microscopic Characterization 2009;43:9519–24.
568 doi:10.1021/es902165y.

569 [24] Boghani HC, Kim JR, Dinsdale RM, Guwy AJ, Premier GC. Control of power sourced
570 from a microbial fuel cell reduces its start-up time and increases bioelectrochemical
571 activity. Bioresour Technol 2013;140:277–85. doi:10.1016/j.biortech.2013.04.087.

572 [25] Kaur A, Boghani HC, Michie I, Dinsdale RM, Guwy AJ, Premier GC. Inhibition of
573 methane production in microbial fuel cells: Operating strategies which select electrogens
574 over methanogens. Bioresour Technol 2014;173:75–81.
575 doi:10.1016/j.biortech.2014.09.091.

576 [26] Wagner RC, Call DF, Logan BE. Optimal Set Anode Potentials Vary in
577 Bioelectrochemical Systems. Environ Sci Technol 2010;44:6036–41.
578 doi:10.1021/es101013e.

579 [27] Zhu X, Yates MD, Hatzell MC, Rao HA, Saikaly PE, Logan BE. Microbial Community
580 Composition Is Unaffected by Anode Potential. Environ Sci Technol 2014;48:1352–8.
581 doi:10.1021/es404690q.

582 [28] Kokko ME, Mäkinen AE, Sulonen MLK, Puhakka JA. Effects of anode potentials on
583 bioelectrogenic conversion of xylose and microbial community compositions. Biochem
584 Eng J 2015;101:248–52. doi:10.1016/j.bej.2015.06.007.

585 [29] Lefebvre O, Shen Y, Tan Z, Uzabiaga A, Chang IS, Ng HY. A comparison of membranes
586 and enrichment strategies for microbial fuel cells. Bioresour Technol 2011;102:6291–4.
587 doi:10.1016/j.biortech.2011.02.003.

[30] Rago L, Monpart N, Cortés P, Baeza JA, Guisasola A. Performance of microbial electrolysis cells with bioanodes grown at different external resistances. Water Sci Technol 2016;73:1129–35. doi:10.2166/wst.2015.418.

[31] Logan BE, Hamelers B, Rozendal R, Schröder U, Keller J, Freguia S, et al. Microbial fuel cells: Methodology and technology. Environ Sci Technol 2006;40:5181–92. doi:10.1021/es0605016.

[32] Kumar G, Bakonyi P, Zhen G, Sivagurunathan P, Koók L, Kim S-H, et al. Microbial electrochemical systems for sustainable biohydrogen production: Surveying the experiences from a start-up viewpoint. Renew Sustain Energy Rev 2017;70:589–97. doi:10.1016/j.rser.2016.11.107.

[33] Hong Y, Call DF, Werner CM, Logan BE. Adaptation to high current using low external resistances eliminates power overshoot in microbial fuel cells. Biosens Bioelectron 2011;28:71–6. doi:10.1016/j.bios.2011.06.045.

[34] Wang X, Feng Y, Ren N, Wang H, Lee H, Li N, et al. Accelerated start-up of two-chambered microbial fuel cells: Effect of anodic positive poised potential. Electrochim Acta 2009;54:1109–14. doi:10.1016/j.electacta.2008.07.085.

[35] Kokko M, Epple S, Gescher J, Kerzenmacher S. Effects of wastewater constituents and operational conditions on the composition and dynamics of anodic microbial communities in bioelectrochemical systems. Bioresour Technol 2018;258:376–89. doi:10.1016/j.biortech.2018.01.090.

[36] Cetinkaya AY, Ozdemir OK, Koroglu EO, Hasimoglu A, Ozkaya B. The development of catalytic performance by coating Pt-Ni on CMI7000 membrane as a cathode of a microbial fuel cell. Bioresour Technol 2015;195:188–93. doi:10.1016/j.biortech.2015.06.064.

[37] Dubois M, Gilles KA, Hamilton J, Rebers PA, Smith F. Colorimetric method for determination of sugars and related substances. Anal Chem 1956;28:350–6.

[38] Haavisto JM, Kokko ME, Lay CH, Puhakka JA. Effect of hydraulic retention time on continuous electricity production from xylose in up-flow microbial fuel cell. Int J Hydrogen Energy 2017;42:27494–501. doi:10.1016/j.ijhydene.2017.05.068.

[39] Van Haandel A, Van der Lubbe J. Handbook biological waste water treatment : design and optimisation of activated sludge systems. Leidschendam: Quist Publishing; 2007.

[40] Muyzer G, de Waal E, Uitterlinden AG. Profiling of complex microbial populations by denaturing gradient gel electrophoresis analysis of polymerase chain reaction-amplified genes coding for 16S rRNA. Appl Environ Microbiol 1993;59:695–700.

[41] Muyzer G, Hottenträger S, Teske A, Wawer C. Denaturing gradient gel electrophoresis of PCR-amplified 16S rRNA – a new molecular approach to analyse the genetic diversity of mixed microbial communities. In: Akkermans ADL, van Elsas JD, de Bruijn F, editors. Mol. Microb. Ecol. Man., Kluwer Academic Publishers; 1996, p. 3.4.4/1-23.

[42] Koskinen P, Kaksonen A, Puhakka J. The Relationship Between Instability of H2 Production and Compositions of Bacterial Communities Within a Dark Fermentation

Fluidized-Bed Bioreactor. Biotechnol Bioeng 2006;97:742–58. doi:10.1002/bit.21299.

[43] Lakaniemi AM, Hulatt C, Thomas D, Tuovinen O, Puhakka J. Biogenic hydrogen and methane production from Chlorella vulgaris and Dunaliella tertiolecta biomass. Biotechnol Biofuels 2011;4:1–12. doi:10.1186/1754-6834-4-34.

[44] Wei J, Liang P, Cao X, Huang XIA. A New Insight into Potential Regulation on Growth and Power Generation of Geobacter sulfurreducens in Microbial Fuel Cells Based on Energy Viewpoint. Environ Sci Technol 2010;44:3187–91. doi:10.1021/es903758m.

[45] Sun D, Call DF, Kiely PD, Wang A, Logan BE. Syntrophic interactions improve power production in formic acid fed MFCs operated with set anode potentials or fixed resistances. Biotechnol Bioeng 2012;109:405–14. doi:10.1002/bit.23348.

[46] Aelterman P, Freguia S, Keller J, Verstraete W, Rabaey K. The anode potential regulates bacterial activity in microbial fuel cells. Appl Microbiol Biotechnol 2008;78:409–18. doi:10.1007/s00253-007-1327-8.

[47] Carmona-Martínez AA, Trably E, Milferstedt K, Lacroix R, Etcheverry L, Bernet N. Long-term continuous production of H2 in a microbial electrolysis cell (MEC) treating saline wastewater. Water Res 2015;81:149–56. doi:10.1016/j.watres.2015.05.041.

[48] Zhu X, Tokash JC, Hong Y, Logan BE. Controlling the occurrence of power overshoot by adapting microbial fuel cells to high anode potentials. Bioelectrochemistry 2013;90:30–5. doi:10.1016/j.bioelechem.2012.10.004.

[49] Mathuriya AS, Sharma VN. Treatment of Brewery Wastewater and Production of Electricity through Microbial Fuel Cell Technology. Int J Biotechnol Biochem 2010;6:71–80.

[50] Lu M, Chen S, Babanova S, Phadke S, Salvacion M, Mirhosseini A, et al. Long-term performance of a 20-L continuous flow microbial fuel cell for treatment of brewery wastewater. J Power Sources 2017;356:274–87. doi:10.1016/j.jpowsour.2017.03.132.

[51] Koók L, Rózsenberszki T, Nemestóthy N, Bélafi-Bakó K, Bakonyi P. Bioelectrochemical treatment of municipal waste liquor in microbial fuel cells for energy valorization. J Clean Prod 2016;112:4406–12. doi:10.1016/j.jclepro.2015.06.116.

[52] Wen Q, Wu Y, Zhao L, Sun Q. Production of electricity from the treatment of continuous brewery wastewater using a microbial fuel cell. Fuel 2010;89:1381–5. doi:10.1016/j.fuel.2009.11.004.

[53] Chandrasekhar K, Venkata Mohan S. Induced catabolic bio-electrohydrolysis of complex food waste by regulating external resistance for enhancing acidogenic biohydrogen production. Bioresour Technol 2014;165:372–82. doi:10.1016/j.biortech.2014.02.073.

[54] Dogan T, Ince O, Oz NA, Ince BK. Inhibition of volatile fatty acid production in granular sludge from a UASB reactor. J Environ Sci Heal - Part A Toxic/Hazardous Subst Environ Eng 2005;40:633–44. doi:10.1081/ESE-200046616.

[55] Bakonyi P, Koók L, Keller E, Bélafi-Bakó K, Rózsenberszki T, Saratale GD, et al. Development of bioelectrochemical systems using various biogas fermenter effluents as

667 inocula and municipal waste liquor as adapting substrate. Bioresour Technol
668 2018;259:75–82. doi:10.1016/j.biortech.2018.03.034.

669 [56] Xia X, Cao X, Liang P, Huang X, Yang S, Zhao G. Electricity generation from glucose by
670 a Klebsiella sp. in microbial fuel cells. Appl Microbiol Biotechnol 2010;87:383–90.
671 doi:10.1007/s00253-010-2604-5.

672 [57] Xu S, Liu H. New exoelectrogen Citrobacter sp. SX-1 isolated from a microbial fuel cell.
673 J Appl Microbiol 2011;111:1108–15. doi:10.1111/j.1365-2672.2011.05129.x.

674 [58] Zhang T, Cui C, Chen S, Yang H, Shen P. The direct electrocatalysis of Escherichia coli
675 through electroactivated excretion in microbial fuel cell. Electrochem Commun
676 2008;10:293–7. doi:10.1016/j.elecom.2007.12.009.

677 [59] Prins RA. Isolation, culture, and fermentation characteristics of Selenomonas ruminantium
678 var. bryanti var. n. from the rumen of sheep. J Bacteriol 1971;105:820–5.

679 [60] Yükselen MA. Preservation characteristics of UASB Sludges. J Environ Sci Heal Part A
680 Environ Sci Eng Toxicol 1997;32:2069–76. doi:10.1080/10934529709376666.

681 [61] Ishii S, Suzuki S, Norden-Krichmar TM, Nealson KH, Sekiguchi Y, Gorby YA, et al.
682 Functionally stable and phylogenetically diverse microbial enrichments from microbial
683 fuel cells during wastewater treatment. PLoS One 2012;7.
684 doi:10.1371/journal.pone.0030495.

685

686

The effect of start-up on energy recovery and compositional changes in brewery wastewater in bioelectrochemical systems

Johanna M. Haavisto[1,*], Marika E. Kokko[1], Aino-Maija Lakaniemi[1], Mira L. K. Sulonen[1,#], Jaakko A. Puhakka[1]

SUPPORTING INFORMATION

[1] *Tampere University, Faculty of Engineering and Natural Sciences, Tampere, Finland*

[#] *Present address: Universitat Autònoma de Barcelona, Departament Química, Biològica i Ambiental, Barcelona, Spain*

* Corresponding author: P.O. Box 541, FI-33104 Tampere University, Finland; E-mail: johanna.haavisto@tuni.fi; Telephone: +358400486070

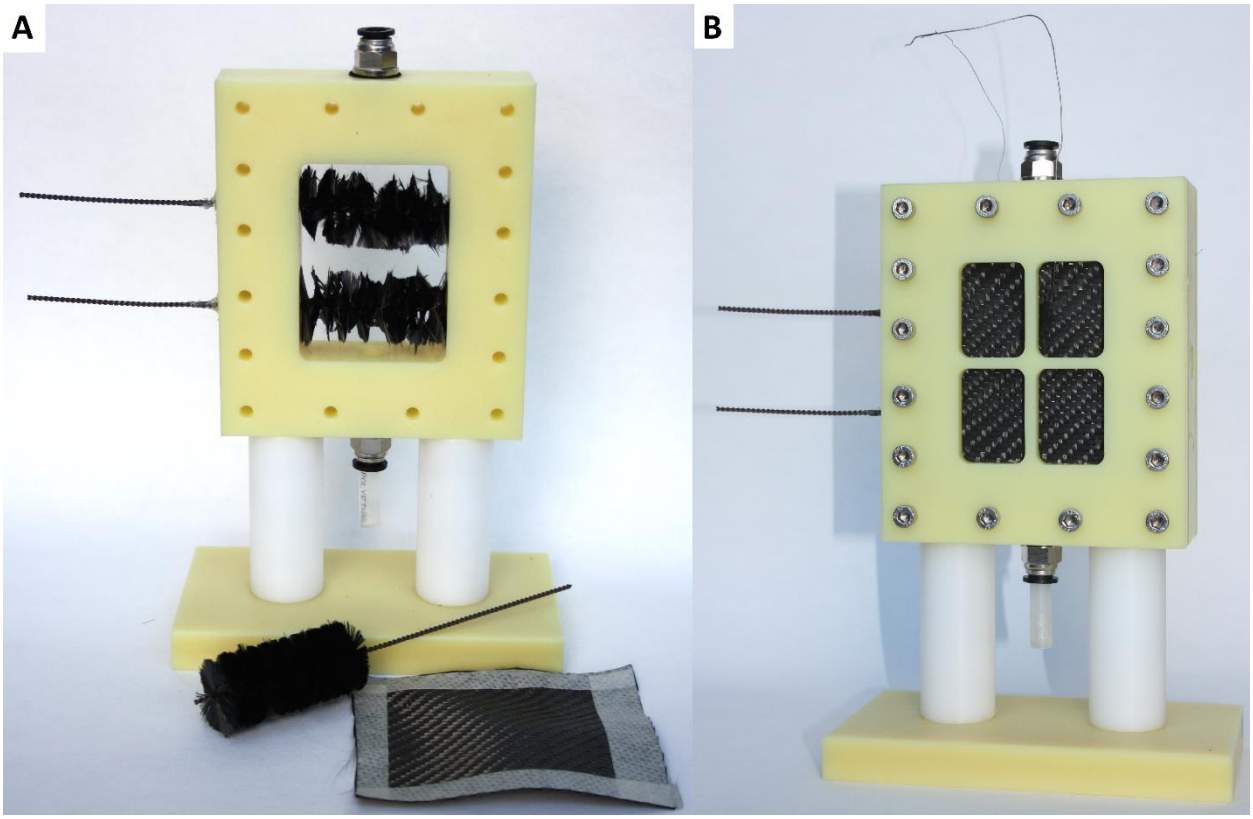

Fig. S1. Photographs of the bioelectrochemical systems with air cathodes A) anode electrode positions and anode (carbon brush) and cathode (carbon cloth) electrode materials and B) bioelectrochamical system with air-cathodes assembled on both sides of the anode chamber. Metallic recirculation tube connections are shown below and above the anode chamber frame in both photos. Reference electrode was positioned in the middle of the anode chamber parallel to the anode electrodes.

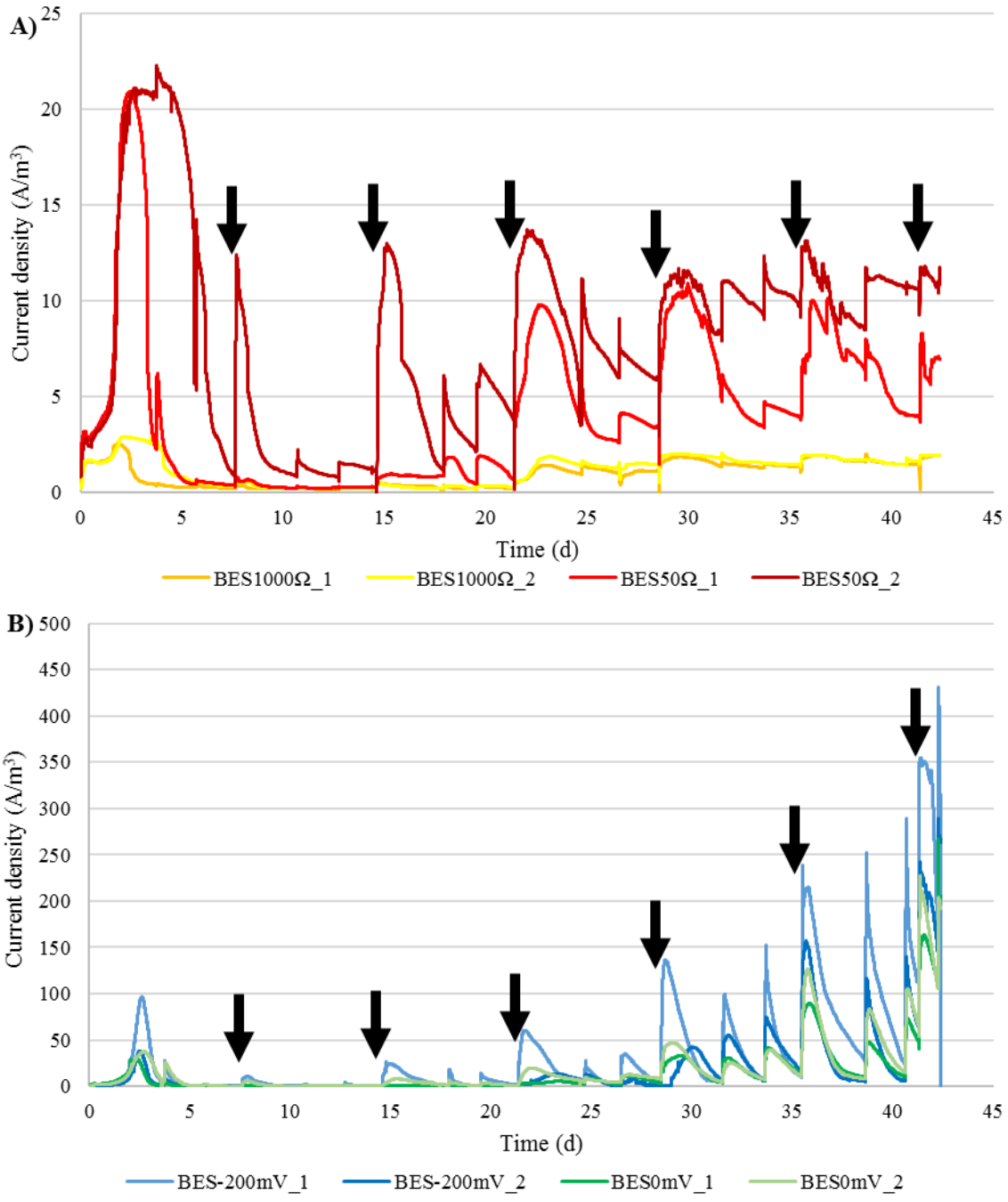

Fig. S2. Current densities of the BESs with A) external resistances and B) adjusted anode potentials during the start-up phase. Black arrows represent the feeding points.

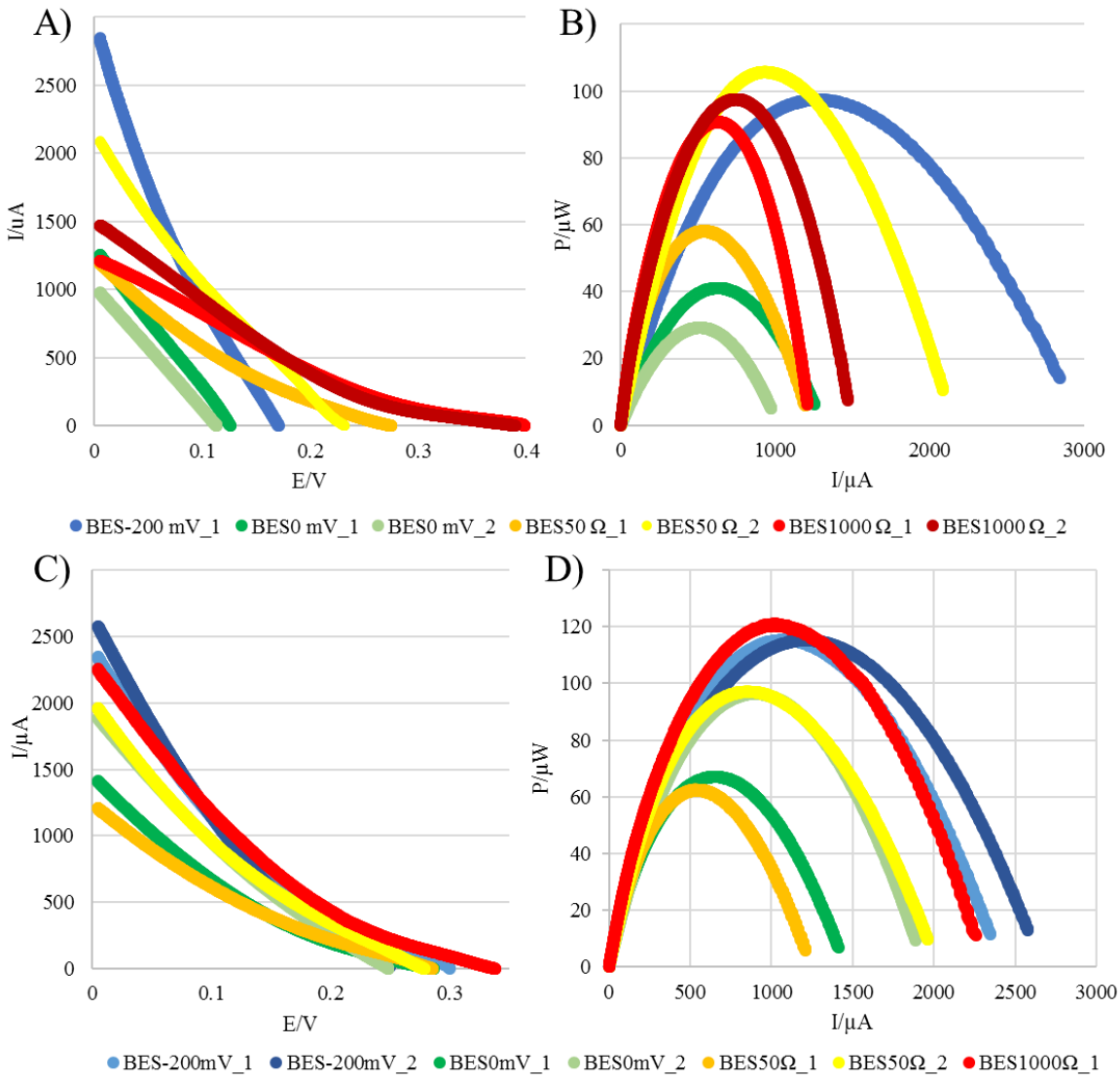

Fig. S3. Whole cell linear sweep voltammetry polarization and power curves of the studied BESs in the end of the start-up phase (A and B) and in the end of the experiment (C and D). Due to connection problems, the results of BES_{-200mV}_2 are not shown in A and B and $BES_{1000\Omega}$_2 in C and D.

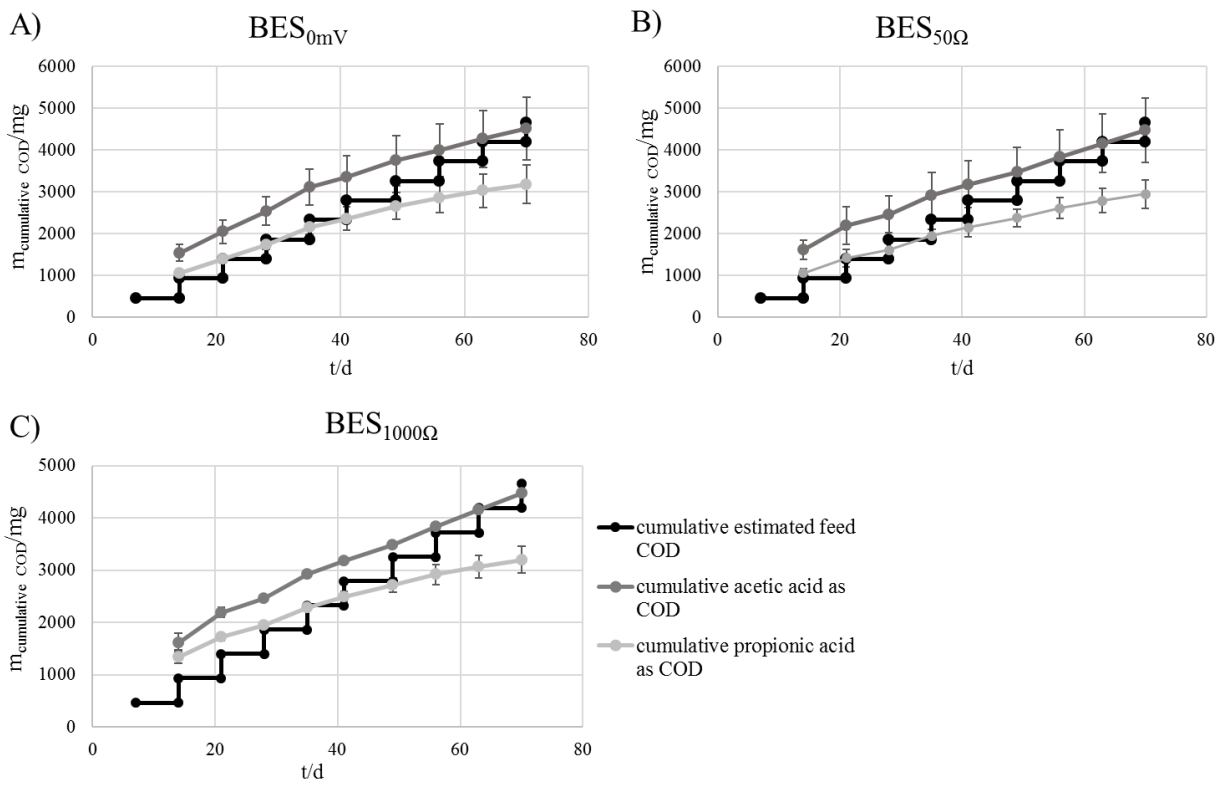

720

721 **Fig. S4.** Cumulative COD in feed, and acetic acid and propionic acid formation as COD
722 equivalents after the first feeding in A) BES_{0mV}, B) $BES_{50\Omega}$ and C) $BES_{1000\Omega}$. Added COD in
723 feed is shown in black as a reference. Higher concentrations of acetic acid and propionic acid
724 compared to fed COD are due to the COD content of anaerobic sludge inoculum.

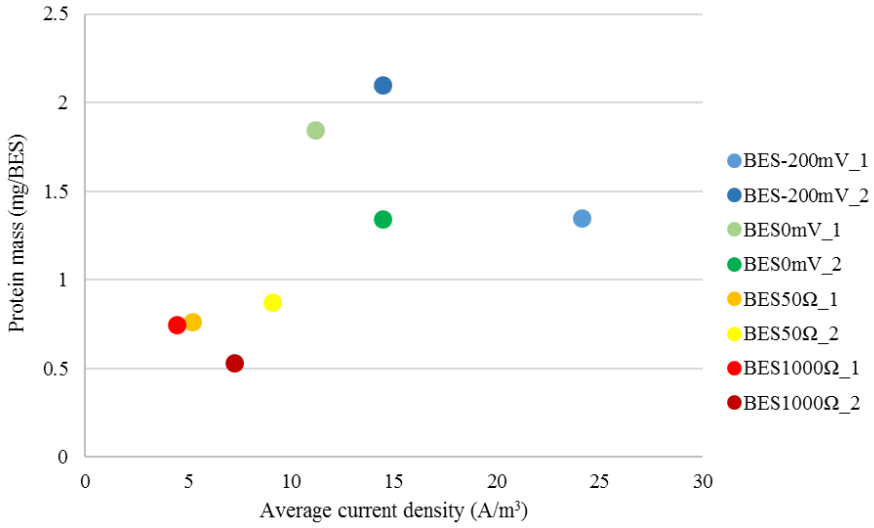

725

726 **Fig. S5.** Dependence of anodic biofilm protein mass on average current density. Average current
727 densities were calculated as mean values of feeding cycles 2-10 between days 7 and 70.

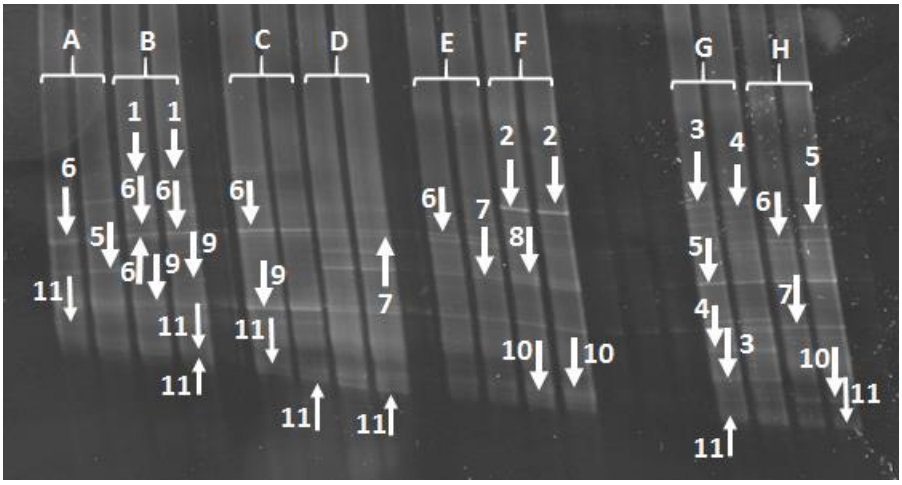

Fig. S6. Denaturing gradient gel electrophoresis profiling of the bioelectrochemical system anode biofilms. Duplicate samples were prepared from each BES: A) and B) BES_{-200mV}, C) and D) BES_{0mV}, E) and F) $BES_{50\Omega}$, and G) and H) $BES_{1000\Omega}$. Bands with same number have similar affiliation (Table S1).

Table S1. Affiliations of the micro-organisms detected from the anode biofilms of brewery wastewater-fed bioelectrochemical systems. The identification was conducted by using polymerase chain reaction denaturing gradient electrophoresis (PCR-DGGE) followed by sequencing. Identification of multiple bands with similar affiliation caused variation in sequence length and similarity presented in the table.

Band label	SL	Sim (%)	Affiliation (acc)	Class/Family	Origin of the sample
1	303-304	98.7-99.0	uncultured bacteroidetes bacterium (JF681276.1)	-/-	thermophilic anaerobic reactor
2	449-472	100	uncultured beta proteobacterium (AB635880.1)	Betaproteobacteria / -	groundwater from deep tube well
3	285-410	98.6-100	*Klebsiella* sp. (MF442345.1)	Gammaproteobacteria / *Enterobacteriaceae*	roots of Brazil nut tree
4	288-400	99.0-99.8	*Citrobacter* sp. (LT556085.1)	Gammaproteobacteria / *Enterobacteriaceae*	
5	463	98.5	uncultured bacterium clone (KC551588.1)	-/-	activated sludge
		97.8	uncultured *Azonexus* sp. (LC001033.1)	Betaproteobacteria / *Azonexaceae*	microbial fuel cell
6	299-469	98.2-100	*Selenomonas* sp. (AB717126.1)	Negativicutes / *Selenomonadaceae*	microbial fuel cell
		98.2-100	*Schwartzia* sp. (GQ332209.1)	Negativicutes / *Selenomonadaceae*	grease hat within grease trap
7	392-417	99.5-99.8	*Escherichia coli* (CP022414.1)	Gammaproteobacteria / *Enterobacteriaceae*	
8	418	99.5	*Geobacter* sp. (JF736650.1)	Deltaproteobacteria / *Geobacteraceae*	microbial fuel cell
9	286-464	96.9-100	*Azospira* sp. (JF736645.1)	Betaproteobacteria / *Rhodocyclaceae*	microbial fuel cell
10	377-399	98.4-99.0	*Desulfovibrio marrakechensis* (KX261411.1)	Deltaproteobacteria / *Desulfovibrionaceae*	Sludge and beet sugar industrial wastewater
		99.5-100	uncultured bacterium clone (KU589101.1)	-/-	UASB reactor
11	350-402	96.9-100	uncultured bacterium clone (EF515442.1)	-/-	microbial fuel cell